

# Studies on Dynamic Characteristics of Sandwich Functionally Graded Plate Subjected to Uniform Temperature Field



E. Amarnath and M. C. Lenin Babu

**Abstract** The effect of uniform temperature on dynamic characteristics of a sandwich plate with functionally graded (FG) core is analyzed by finite element methods. The top and bottom of the sandwich plate are considered as metal and ceramic, and the core is considered as functionally graded. Aluminum and alumina materials are used as top and bottom face sheets, and the same materials are graded through thickness for FGM core. The material properties of FG core vary throughout the thickness direction according to the power law index. The effective material properties are calculated using the Voigt technique. The Buckling temperature of sandwich plate is analyzed for different boundary conditions and used as criteria to study the effect of temperature on natural frequencies and mode shapes.

**Keywords** Free vibration · Sandwich functionally graded plate · Thermal environment · First-order shear deformation theory

## 1 Introduction

Functionally graded materials (FGM) concept was introduced in 1984 by Japan for aircraft designs. FGM are the class of composites which continuously change properties throughout its thickness direction. FGM are widely preferred in automobile and aerospace industries because of their strength, corrosion resistance, and thermal barrier capabilities. Gasik [1] reviewed different micro mechanical modeling approaches and discussed about the problems involving in the design of functionally graded materials. Victor and Larry [2] reviewed FGM structures with the viewpoint of dynamic characteristics and various manufacturing methods. Udupa et al. [3] overviewed the various concepts involved in designing of functionally graded composites and their applications. Watanabe [4] studied about the fabrication of functionally gradient materials by powder metallurgical processing technique and

---

E. Amarnath · M. C. L. Babu (✉)

School of Mechanical and Building Sciences, VIT, Chennai 600127, Tamil Nadu, India

e-mail: [lenin\\_babu@yahoo.com](mailto:lenin_babu@yahoo.com)

© Springer Nature Singapore Pte Ltd. 2021

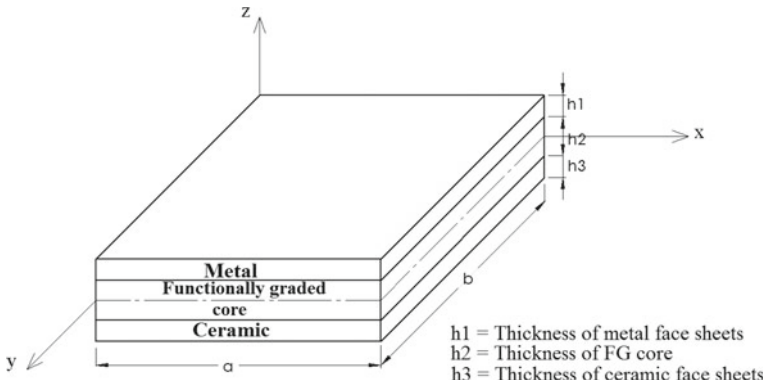
S. Dutta et al. (eds.), *Advances in Structural Vibration*, Lecture Notes

in Mechanical Engineering, [https://doi.org/10.1007/978-981-15-5862-7\\_5](https://doi.org/10.1007/978-981-15-5862-7_5)

showed it provides a wide range of compositional and microstructural control along-with shape forming capability. Thai and Kim [5] critically reviewed FG plates by considering modeling and loading methods as criteria. Zhao et al. [6] investigated the thermal buckling behavior of functionally graded plates numerically, and the plate was modeled using first-order shear deformation theory (FSDT). Influence of volume fraction and hole geometry on buckling load was also analyzed by them. Kiani et al. [7] studied the thermal and mechanical instability of the sandwich functionally graded plate when resting on the elastic base. Zenkour and Mashat [8] investigated the thermal buckling behaviour of functionally graded plate (FGP) by considering the effects of shear deformation and thickness stretching. Bouhadra et al. [9] calculated the thermal buckling temperature of FGP with uniform temperature. In their FGP model, the material distribution was considered by power law index and Voigt mode, and varied throughout the thickness direction of the plate. Numerical analysis was carried to study the effect of plate aspect ratio and power law index on critical buckling temperature. Reza [10] did a detailed investigation about a thermal buckling of beams, plates, and shells. Bhagat et al. [11] determined the thermal buckling and natural frequency of uniformly heated isotropic cylindrical shell. Mayandi and Jeyaraj [12] investigated about the buckling and natural frequency of composite beam under non-uniform thermal load. Jeyaraj et al. [13] discussed about the vibration and acoustic characteristics of the viscoelastic sandwich plate under the thermal environment. Li et al. [14] considered two different types of sandwich functionally graded plates to study the free vibration characteristics by three dimensional theory of elasticity. Simply supported and clamped boundary conditions were used to find the free vibration characteristics under the influence of volume fraction, thickness-length ratios, aspect ratio, and layer thickness ratios of sandwich FGP. Chandra et al. [15] determined the analytical solution for vibration and acoustic response of FGP by using FSDT. They showed that the increase in power law index leads to a decrease in natural frequency for simply supported boundary condition. Jeyaraj et al. [16] found that the vibration and acoustic properties of steel plate are significantly affected by the temperature. For this study, they have used critical buckling temperature as a parameter. In this work, a sandwich functionally graded plate is considered to study the effect of uniform temperature influences on free vibration characteristics. By using power law index, material properties varied throughout the thickness direction on functionally graded core. The effective properties are determined by using the Voigt technique. Influence of power law, different boundary conditions (CCCC, CCFC, FCFC, and CFFC), and temperature rise on mode shapes and natural frequencies is also studied in detail.

## 2 Problem Description

A sandwich plate with functionally graded core is considered for this study with top and bottom face sheets considered to be metal and ceramic as shown in Fig. 1.



**Fig. 1** Sandwich plate

Volume fraction of alumina ( $V_c$ ) across the thickness direction is given in Eq. 1, where  $p$  denotes power law index,  $z$  is the height of each layer from the mid plane, and  $h$  the total thickness of the plate along  $z$  coordinates is  $h$ .

$$V_c = \left(0.5 + \frac{z}{h}\right)^p \tag{1}$$

$$V_m = (1 - V_c) \tag{2}$$

$$P(z) = (P_c - P_m)V_m + P_m \tag{3}$$

Effective Young’s modulus ( $E$ ), density( $\rho$ ), Poisson’s ratio ( $\nu$ ), and coefficient of thermal expansion ( $\alpha$ ) were derived using the Voigt model as given in Eq. 3, where  $c$  and  $m$  denote ceramic and metal, respectively. In this work, four different sandwich configurations such as 4-2- 4, 3-4-3, 2-6-2, and 1-8-1 are considered to get critical buckling temperature. In each configuration, the numbers represent the metal face sheet thickness ( $h_1$ ), FG core thickness ( $h_2$ ), and ceramic face sheet thickness ( $h_3$ ) of the sandwich FGP.

### 3 Methodology

As given in the equation critical thermal buckling temperature is calculated with considering the pre-stress effects [12]

$$([K_{ss}] + \lambda_i [K_{gs}])\{\psi_i\} = 0 \tag{4}$$

where  $[K_{ss}]$  denotes structural stiffness matrix,  $[K_{gs}]$  is geometric stiffness,  $\lambda_i$  is the eigenvalue, and  $\Psi_i$  is the eigenvector. Then the natural frequencies and mode shapes were analyzed by assuming the critical buckling temperature as a parameter. The effect of temperature is included in the form of the geometric stiffness matrix as shown in Eq. 5.

$$(([K_{ss}] + [K_{gs}]) - \omega_i^2[M])\{\Phi_i\} = 0 \tag{5}$$

where  $\omega_i$  denotes natural frequencies and  $[M]$  is structural mass matrix. Finally, the influence of power law index on critical buckling temperature and free vibration characteristics are analyzed for different boundary conditions like CCCC, CCFC, FCFC, and CFFC. The entire analysis carried out by using ANSYS finite element software.

### 4 Validation Studies

Bouhadra et al. [9] analyzed critical buckling temperature for Al/Al<sub>2</sub>O<sub>3</sub> FGP and Li et al. [14] examined non-dimensional natural frequencies of sandwich FGP. These two cases are used for validating the above finite element formulation. The physical properties of Al and Al<sub>2</sub>O<sub>3</sub> are given in Table 1.

Validation of critical buckling temperature on FGP is presented in Table 2, and non-dimensional natural frequencies of sandwich FGP are shown in Table 3. The present study shows good agreement with the results considered for validation.

**Table 1** Physical properties of Alumina (Al<sub>2</sub>O<sub>3</sub>) and Aluminum (Al)

Properties	Ceramic (Alumina)	Metal (Aluminum)
Young’s modulus, GPa	380	70
Poisson’s ratio	0.3	0.3
Density, kg/m <sup>3</sup>	3800	2707
Coefficient of thermal expansion, 1/°C	$7.4 \times 10^{-6}$	$23 \times 10^{-6}$

**Table 2** Validation of critical buckling temperature of all side clamped square FGP

a/h	Theory	p = 0	p = 0.5	p = 1	p = 2	p = 5
50	Bouhadra et al. [9]	181.3	102.7	84.3	74.7	76.9
	Present study	180.7	102.7	84.1	74.4	76.4
100	Bouhadra et al. [9]	45.5	25.8	21.156	18.7	19.3
	Present study	45.4	25.8	21.121	18.6	19.2

**Table 3** Validation of non-dimensional natural frequency of clamped square sandwich FGP

h/a	Theory	p = 0.5	p = 1	p = 2	p = 5	p = 10
0.01	Li et al. [14]	2.45	2.54	2.64	2.80	2.91
	Present study	2.42	2.5	2.61	2.76	2.87
0.1	Li et al. [14]	2.24	2.34	2.45	2.60	2.70
	Present study	2.21	2.32	2.43	2.58	2.67
0.2	Li et al. [14]	1.86	1.97	2.09	2.22	2.28
	Present study	1.83	1.96	2.07	2.20	2.27

## 5 Results and Discussion

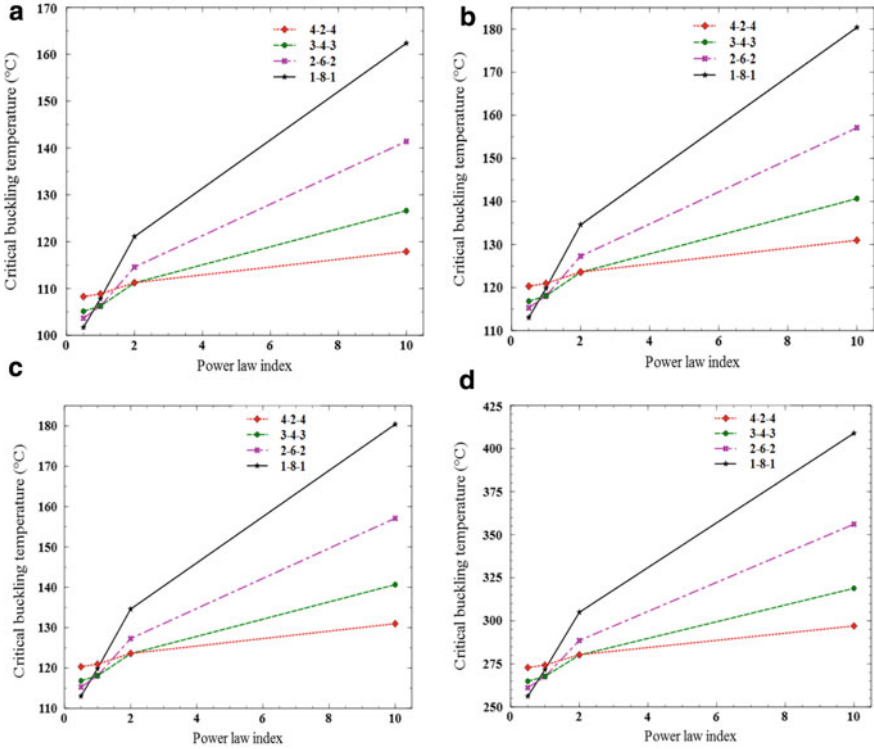
A rectangular sandwich FGP having dimensions of (0.5 × 0.4 × 0.01)m corresponding to length, width, and thickness directions is considered for the detailed study. After a careful examination, a converged 45 × 45 finite element mesh size is used.

### 5.1 Critical Buckling Temperature

Critical buckling temperature is analyzed for different power law indexes, boundary conditions, and core thicknesses as shown in Figs. 2b–d. It is clear that an increase in power law index tends to an increase in critical buckling temperature because of the increase in stiffness due to the ceramic content. From Fig. 2a, one can see that at a lower power law index, the critical buckling temperature is high for 4-2-4 configuration with CCCC boundary condition. In contrast to the above at higher power law index, the critical buckling temperature is found to be high for 1-8-1 configuration. This is due to the variation of ceramic content in different configurations considered for the analysis. Figures 2b–d shows the variation of critical buckling temperature of sandwich FGP for CCFC, FCFC, and CFFC boundary conditions. It is clear that the variation of thermal buckling strength in other boundary conditions is following the trend of CCCC and indicates higher strength for CFFC condition. This may be due to the free expansion of adjacent free edges.

### 5.2 Free Vibration Characteristics

In order to show the influence of temperature on free vibration characteristics, it is decided to use 1-8-1 sandwich FGP configuration since it shows higher thermal buckling strength than others. Then the obtained critical buckling temperature is used as a parameter and applied over all the nodes of the plate uniformly. For this



**Fig. 2** Critical buckling temperature,  $T_{cr}$  ( $^{\circ}C$ ) for different boundary conditions

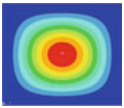
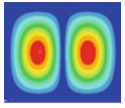
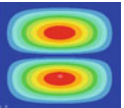
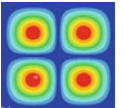
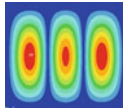
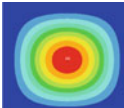
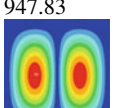
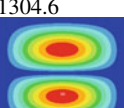
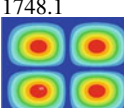
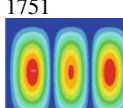
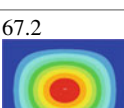
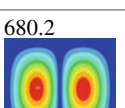
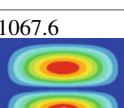
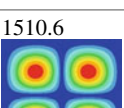
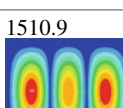
purpose,  $0 \cdot T_{cr}$ ,  $0.25 \cdot T_{cr}$ ,  $0.5 \cdot T_{cr}$ ,  $0.75 \cdot T_{cr}$  and  $0.99 \cdot T_{cr}$  uniform temperature rise are considered. Then the natural frequencies are obtained by performing the modal analysis by considering pre-stress effects due to the applied temperature. Effect of temperature on natural frequencies of sandwich FGP for different boundary conditions, power law indexes, and uniform temperature rises is shown in Tables 4, 6, 8 and 10. From Table 4, one can see that the natural frequencies are increasing with an increase in power law index. It is due to the increase in ceramic content than metal and leads to an increase in stiffness of sandwich FGP. At the same time, Table 4 shows that the natural frequencies are decreased when the applied temperature is increased. This may be due to the influence of pre-stress effect on bending stiffness. A similar kind of variation is observed in other boundary conditions also and showed in Tables 6, 8, and 10.

Next, the influences of uniform temperature rise on mode shapes is studied for different boundary conditions. The analysis has been done for different power law indexes; however, for power law index 1, the material properties are varying linearly with respect to thickness. So in this study, only the power law 1 is chosen to study the effect of temperature on free vibration characteristics. Tables 5, 7, 9, and 11 show the results of the effect of temperature on the first five mode shapes for different

**Table 4** Comparison of natural frequencies for (1-8-1) sandwich FGP with CCCC boundary condition

Power law	T <sub>cr</sub> (°C)	Uniform temp rise	First mode	Second mode	Third mode	Fourth mode	Fifth mode
0.5	101.7	0*T <sub>cr</sub>	635.4	1115.1	1452.8	1889.2	1894.7
		0.25*T <sub>cr</sub>	552.5	1020	1359.2	1790.2	1794.5
		0.5*T <sub>cr</sub>	453.2	914.3	1258	1685.1	1688
		0.75*T <sub>cr</sub>	322.2	793.6	1147.3	1572.4	1574.1
		0.99*T <sub>cr</sub>	64.8	655.9	1029.2	1455.6	1456.2
1	107.8	0*T <sub>cr</sub>	658.4	1155.9	1506.4	1959.5	1965.1
		0.25*T <sub>cr</sub>	572.5	1057.3	1409.3	1857	1861.2
		0.5*T <sub>cr</sub>	469.6	947.8	1304.6	1748.1	1751
		0.75*T <sub>cr</sub>	333.8	822.8	1189.9	1631.5	1633
		0.99*T <sub>cr</sub>	67.2	680.2	1067.6	1510.6	1510.9
10	162.3	0*T <sub>cr</sub>	755.6	1326.8	1729.3	2249.8	2256.2
		0.25*T <sub>cr</sub>	657	1213.6	1617.9	2132.1	2136.9
		0.5*T <sub>cr</sub>	538.9	1087.9	1497.6	2007	2010.3
		0.75*T <sub>cr</sub>	383	944.4	1365.9	1873.1	1874.9
		0.99*T <sub>cr</sub>	76.9	780.7	1225.5	1734.2	1734.6

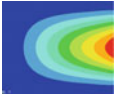
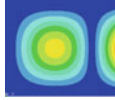
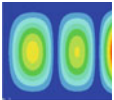
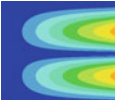
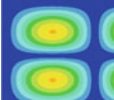
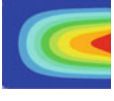
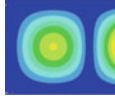
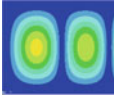
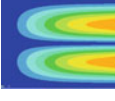
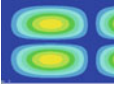
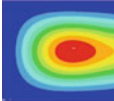
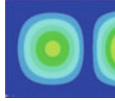
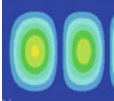
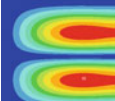
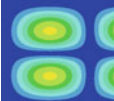
**Table 5** Mode shapes variation of sandwich FGP with uniform temperature rise by CCCC (1-8-1)

Uniform temp	First mode	Second mode	Third mode	Fourth mode	Fifth mode
0*T <sub>cr</sub>	658.4 	1155.9 	1506.4 	1959.5 	1965.1 
0.5*T <sub>cr</sub>		947.83 	1304.6 	1748.1 	1751 
0.99*T <sub>cr</sub>	67.2 	680.2 	1067.6 	1510.6 	1510.9 

**Table 6** Comparison of natural frequencies for (1-8-1) sandwich FGP with CCFC boundary condition

Power law	T <sub>cr</sub> (°C)	Uniform temp rise	First mode	Second mode	Third mode	Fourth mode	Fifth mode
0.5	113	0*T <sub>cr</sub>	494.7	700.1	1177	1327.2	1552.9
		0.25*T <sub>cr</sub>	435	636.7	1114.4	1248.3	1471.2
		0.5*T <sub>cr</sub>	361.7	565.8	1047.4	1161.7	1384.7
		0.75*T <sub>cr</sub>	261.4	484.5	975.2	1065	1292.6
		0.99*T <sub>cr</sub>	53.4	391.4	899.8	959.5	1197.8
1	119.8	0*T <sub>cr</sub>	512.5	725.5	1220.1	1376	1610.4
		0.25*T <sub>cr</sub>	450.7	659.8	1155.3	1294.3	1525.7
		0.5*T <sub>cr</sub>	374.8	586.4	1085.9	1204.6	1436.2
		0.75*T <sub>cr</sub>	270.8	502.2	1011.1	1104.5	1340.8
		0.99*T <sub>cr</sub>	55.4	405.8	933.1	995.2	1242.6
10	180.3	0*T <sub>cr</sub>	588.2	832.7	1400.7	1579.6	1848.8
		0.25*T <sub>cr</sub>	517.3	757.3	1326.2	1485.8	1751.6
		0.5*T <sub>cr</sub>	430.1	673	1246.6	1382.8	1648.8
		0.75*T <sub>cr</sub>	310.7	576.4	1160.7	1267.8	1539.3
		0.99*T <sub>cr</sub>	63.5	465.8	1071.1	1142.5	1426.5

**Table 7** Mode shapes variation of sandwich FGP with uniform temperature rise by CCFC (1-8-1)

Uniform temp	First mode	Second mode	Third mode	Fourth mode	Fifth mode
0*T <sub>cr</sub>	512.5 	725.57 	1220.1 	1376 	1610.4 
0.5*T <sub>cr</sub>	374.8 	586.4 	1086 	1204.6 	1436.2 
0.99*T <sub>cr</sub>	55.9 	405.9 	933.1 	995.3 	1242.7 

boundary conditions. Results show the movement of nodes and antinodes is not much significant for CCCC boundary conditions under the influence of temperature. This may be due to its symmetry boundary conditions about x-direction and y-direction. However, this is not true for CCFC boundary condition, first and fourth



**Table 8** Comparison of natural frequencies for (1-8-1) sandwich FGP with FCFC boundary condition

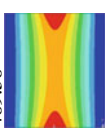
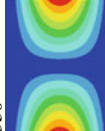
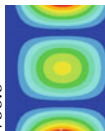
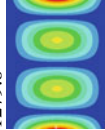
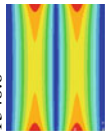
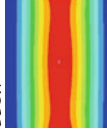
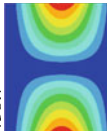
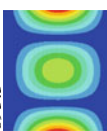
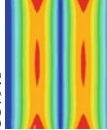
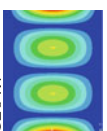
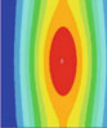
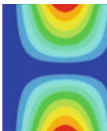
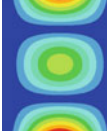
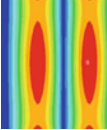
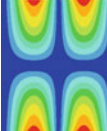
Power law	T <sub>cr</sub> (°C)	Uniform temp rise	First mode	Second mode	Third mode	Fourth mode	Fifth mode
0.5	111.9	0*T <sub>cr</sub>	472.5	530.8	758.9	1234.5	1300.8
		0.25*T <sub>cr</sub>	412.3	480.5	715.3	1198.9	1222.5
		0.5*T <sub>cr</sub>	339.5	423.3	668.9	1137.6	1162
		0.75*T <sub>cr</sub>	242.3	355.8	618.9	1044.5	1123.8
		0.99*T <sub>cr</sub>	48.8	274.1	566.9	944.9	1077.3
1	118.6	0*T <sub>cr</sub>	489.5	550	786.6	1279.8	1348.6
		0.25*T <sub>cr</sub>	427.2	497.9	741.5	1242.9	1267.5
		0.5*T <sub>cr</sub>	351.7	438.7	693.3	1179.6	1204.7
		0.75*T <sub>cr</sub>	251	368.7	641.6	1083.1	1165.1
		0.99*T <sub>cr</sub>	50.6	284.1	587.7	980.03	1117.4
10	178.6	0*T <sub>cr</sub>	561.8	631.3	902.9	1469.3	1548.2
		0.25*T <sub>cr</sub>	490.3	571.5	851.1	1426.9	1455
		0.5*T <sub>cr</sub>	403.7	503.5	795.9	1354.1	1383.1
		0.75*T <sub>cr</sub>	288.1	423.2	736.5	1243.3	1337.6
		0.99*T <sub>cr</sub>	58.2	326.1	674.7	1125	1282.8

modes, antinodes are moving toward the clamped edge from the free edge, and for second, third, and fifth modes, no significant effects of shifting occur as seen from Table 7. Similarly, for FCFC boundary condition, it has been observed that second and third modes are not affected much than other modes. Antinodes are moving toward the center from the free boundaries for the first mode, and the modes are swapped between fourth and fifth modes when the temperature is increased which can be seen from Table 9. Nodes and antinodes of CFFC boundary condition are moving toward the fixed edge corner from the free edge corner for the first mode. This may be due to the free expansion of adjacent free edges. However, one cannot observe a similar variation for other modes except minor shifting.

## 6 Conclusion

The effect of uniform temperature field on dynamic characteristics of rectangular sandwich plate with functionally graded core material is analyzed using finite element methods. Critical buckling temperature and free vibration characteristics of sandwich FGP for temperature rise, material distribution, and different boundary conditions (CCCC, CCFC, FCFC, and CFFC) are studied in detail. It is clear from the results when the power law increases, natural frequencies are increased irrespective of applied temperature. The natural frequencies are decreased when the applied

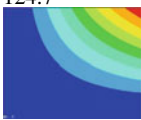
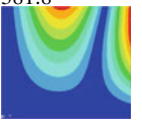
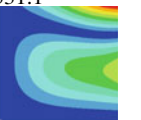
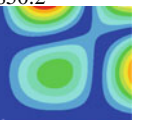
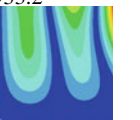

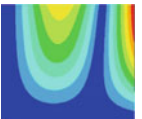
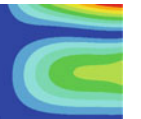
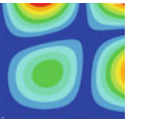
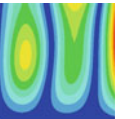
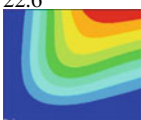
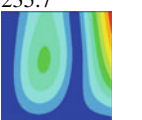
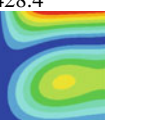
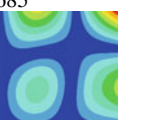
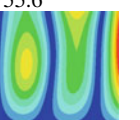
**Table 9** Mode shapes variation of sandwich FGP with uniform temperature rise by FCFC (1-8-1)

Uniform temp	First mode	Second mode	Third mode	Fourth mode	Fifth mode
0* $T_{cr}$	489.58 	550 	786.6 	1279.8 	1348.6 
0.5* $T_{cr}$	351.7 	438.7 	693.3 	1179.6 	1204.7 
0.99* $T_{cr}$	50.6 	284.1 	587.7 	980 	1117.4 

**Table 10** Comparison of natural frequencies for (1-8-1) sandwich FGP with CFFC boundary condition

Power law	T <sub>cr</sub> (°C)	Uniform temp rise	First mode	Second mode	Third mode	Fourth mode	Fifth mode
0.5	256.2	0*T <sub>cr</sub>	120.4	368.5	512.6	820.3	900.6
		0.25*T <sub>cr</sub>	113.4	349.2	496.7	786.3	870
		0.5*T <sub>cr</sub>	103.3	322.8	476.3	748.2	832.6
		0.75*T <sub>cr</sub>	85.4	284.5	449.3	705.8	785.7
		0.99*T <sub>cr</sub>	21.8	227.4	413.4	660.6	729
1	271.6	0*T <sub>cr</sub>	124.7	381.8	531.1	850.2	933.2
		0.25*T <sub>cr</sub>	117.5	361.8	514.5	815	901.5
		0.5*T <sub>cr</sub>	107	334.5	493.5	775.6	862.8
		0.75*T <sub>cr</sub>	88.4	294.8	465.5	731.7	814.3
		0.99*T <sub>cr</sub>	22.6	235.7	428.4	685	755.6
10	408.8	0*T <sub>cr</sub>	143.2	438.2	609.5	976	1071.3
		0.25*T <sub>cr</sub>	134.8	415.2	590.5	935.6	1034.9
		0.5*T <sub>cr</sub>	122.7	383.9	566.4	890.4	990.3
		0.75*T <sub>cr</sub>	101.4	338.3	534.3	839.9	934.7
		0.99*T <sub>cr</sub>	25.9	270.5	491.8	786.3	867.4

**Table 11** Mode shapes variation of sandwich FGP with uniform temperature rise by CFFC (1-8-1)

Uniform temp	First mode	Second mode	Third mode	Fourth mode	Fifth mode
0*T <sub>cr</sub>	124.7 	381.8 	531.1 	850.2 	933.2 
0.5*T <sub>cr</sub>	107 	334.5 	493.5 	775.6 	862.8 
0.99*T <sub>cr</sub>	22.6 	235.7 	428.4 	685 	755.6 

uniform temperature approaches critical buckling temperature. Also, the influences of temperature rise on mode shapes are studied for different boundary conditions. Results showed that the temperature rise significantly altered the mode shape patterns. Among all boundary conditions considered, FCFC showed much variation in the shifting of antinodes and nodes under the influence of temperature.

## References

1. Gasik MM (1998) Micromechanical modelling of functionally graded materials. *Computat Mater Sci* 13:42–55
2. Birman V, Byrd LW (2007) Modeling and analysis of functionally graded materials and structures. *Appl Mech Rev* 60:195–216
3. Udupa G, Shrikantha Rao S, Gangadharan KV (2014) Functionally graded composite materials: an overview. *Procedia Mater Sci* 5:1291–1299
4. Watanabe R (1995) Powder processing of functionally gradient materials. *MRS Bulletin*, 32–34
5. Thai H-T, Kim S-E (2015) A review of theories for the modeling and analysis of functionally graded plates and shells. *Compos Struct* 128:70–86
6. Zhao X, Lee Y, Liew KM (2009) Mechanical and thermal buckling analysis of functionally graded plates. *Compos Struct* 90:161–171
7. Kiani Y, Bagherizadeh E, Eslami MR (2011) Thermal and mechanical buckling of sandwich plates with FGM face sheets resting on the Pasternak elastic foundation. *J Mech Eng* 226:32–41
8. Zenkour AM, Mashat DS (2010) Thermal buckling analysis of ceramic-metal functionally graded plates. *Natural Sci* 2(9):968–978
9. Bouhadra A, Benyoucef S, Tounsi A, Bernard F, Bouiadjra RB, Ahmed Houari MS (2015) Thermal buckling response of functionally graded plates with clamped boundary conditions. *J Thermal Stresses* 38:630–650
10. Reza Eslami M (2018) Buckling and postbuckling of beams, plates, and shells. Springer Nature
11. Bhagat V, Jeyaraj P, Murigendrappa SM (2015) buckling and free vibration characteristics of a uniformly heated isotropic cylindrical panel. *Procedia Eng* 144:474–481. 12th International conference on vibration problems, ICOVP 2015
12. Mayandi K, Jeyaraj P (2013) Bending, buckling and free vibration characteristics of FG-CNT-reinforced polymer composite beam under non-uniform thermal load. *J Mater: Design Appl* 229:13–28
13. Jeyaraj P, Padmanabhan C, Ganesan N (2011) Vibro-acoustic behavior of a multilayered viscoelastic sandwich plate under a thermal environment. *J Sandwich Struct Mater* 13:509–537
14. Li Q, Iu VP, Kou KP (2008) Three-dimensional vibration analysis of functionally graded material sandwich plates. *J Sound Vibr* 311:498–515
15. Chandra N, Raja S, Nagendra Gopal KV (2014) Vibro-acoustic response and sound transmission loss analysis of functionally graded plates. *J Sound Vib* 333: 5786–5802
16. Jeyaraj P, Padmanabhan C, Ganesan N (2008) Vibration and Acoustic response of an isotropic plate in a thermal environmental. *J Vibr Acoust* 130:1–6